Journal of Power Sources 196 (2011) 3420–3425

Contents lists available at ScienceDirect

Journal of Power Sources

journal homepage: www.elsevier.com/locate/jpowsour

Identifying battery aging mechanisms in large format Li ion cells

Matthieu Dubarry[a], Bor Yann Liaw[a,*], Mao-Sung Chen[b], Sain-Syan Chyan[c], Kuo-Chang Han[c], Wun-Tong Sie[c], She-Huang Wu[b]

[a] Hawaii Natural Energy Institute, SOEST, University of Hawaii at Manoa, Honolulu, HI 96822, USA
[b] Department of Materials Engineering, Tatung University, 40 Chungshan N. Rd., Sec. 3, Taipei 104, Taiwan
[c] Chung-Shan Institute of Science and Technology, 481 Jia An Sec., Zhongzheng Rd., Longtan Township, Taoyuan 325, Taiwan

ARTICLE INFO

Article history:
Received 1 April 2010
Received in revised form 2 June 2010
Accepted 10 July 2010
Available online 17 July 2010

Keywords:
Large format
$LiFePO_4$ batteries
Incremental capacity analysis
Thermal degradation
High temperature effect
Loss of lithium inventory

ABSTRACT

Large format $LiFePO_4$-based Li-ion batteries are rapidly becoming available from commercial cell manufacturers. In this paper two types of 10 Ah single cells (one prismatic and another cylindrical) from two manufacturers were tested at room temperature and 60 °C. Both cells suffered severe degradation at 60 °C. The results were analyzed using incremental capacity analysis (ICA) along with other electrochemical techniques. Overall the two types of cells were similar in behavior, despite subtle differences in performance. This study shed some light on the degradation process associated with these two large format $LiFePO_4$ cell designs with regard to thermal degradation at elevated temperatures. The analysis illustrates a unique capability of using ICA to differentiate cell performance and material utilization in different cell designs.

1. Introduction

The pioneer work by Padhi et al. [1] has made olivine-structured $LiFePO_4$ (LFP) battery a competitive energy storage device for smart grid or electric vehicle applications [2–4] along with those based on $LiMn_2O_4$ (spinel), $LiCoO_2$, $LiNiO_2$, or $LiNi_{1/3}Co_{1/3}Mn_{1/3}O_2$ (layer-structured) chemistries [5–8]. Nevertheless, significant capacity degradation has been reported when LFP cells were cycled at elevated temperatures [9,10], suggesting problems with iron dissolution in acidic conditions in $LiPF_6$ electrolytes [9–12] and subsequent deposition of iron on the surface of negative electrode. This iron deposit was believed to act as a catalyst in promoting growth of SEI layer [9]. It was also suggested that some parasitic reaction might occur at high voltages, due to decomposition of electrolyte [13] leading to wetting problems in the electrodes and loss of active material.

The identification of aging and degradation mechanisms in a battery in real-life operation has been a long-desired yet challenging goal in battery R&D and practical applications. Battery aging and degradation often encounter multiple complex and coupled physical–chemical processes in complicated operating conditions, including dynamic duty cycles, temperature/thermal effects, time between operations, and other environmental factors. To quantify aging and degradation effect accurately is not a simple task either. Even if a vigorous test plan can reveal how much capacity is lost in a life cycle test, the result is insufficient to either provide detailed information on degradation mechanism or predict how much loss will occur under a different regime. Only recently incremental capacity analysis (ICA) was demonstrated [14,15] to be explicitly capable of identifying degradation mechanism in combination with high fidelity and accurate computer model simulation. In this work, advancement in applying ICA to decipher aging and degradation mechanisms on large format commercial LFP cells is illustrated.

In previous studies [14,15] in situ, non-invasive electrochemical techniques, including ICA, have been illustrated very powerful in providing detailed information to identify degradation in LFP cells, primarily due to loss of lithium inventory followed by loss of active material [14]. The same techniques can be effective in revealing electrode designs, including grain size and dopant effects [15] in the positive electrode. In this study, origins of capacity loss in degradation in two types of large format (>10 Ah) commercial LFP cells were investigated. The degradation mechanisms at the elevated temperature were discussed.

2. Experimental

Two types of large format (>10 Ah) LFP cells, denoted as "Cell L" and "Cell P", were purchased from two manufacturers, respectively. Table 1 summarizes the specifications for the cells. Cell testing was

* Corresponding author. Tel.: +1 808 956 2339; fax: +1 808 956 2336.
E-mail address: bliaw@hawaii.edu (B.Y. Liaw).

0378-7753/$ – see front matter © 2010 Elsevier B.V. All rights reserved.
doi:10.1016/j.jpowsour.2010.07.029

Table 1
Specifications of the commercial cells used in the study.

Specifications	Cell Label	
	Cell L	Cell P
Shape and geometry	Cuboids (7 cm × 3.5 cm × 8 cm)	Cylinder (H: 13.5 cm, d: 4 cm)
Weight	410 g	380 g
Working potential	3.3 V	3.4 V
Rated capacity	10 Ah	10 Ah
Cell assembly	Flat plates jelly-rolled and interconnected	Cylindrically wound
Vendors	Taiwan	Taiwan

performed by the Energy Storage Materials Laboratory of Tatung University in Taiwan using a multichannel battery tester (GBT-2001i, GW INSTEK). An initial characterization was conducted to assess if all cells from the manufactures were uniform in performance. The regimen used in the initial characterization began with a C/10 charge regime, followed by a 3-h rest, and then a C/10 discharge regime to assess the capacity of the cells. Subsequently, 5 C/2 cycles were executed to condition the cells and determine their rated capacity. The results of the characterization provide the baseline performance of the cells. The resolution of the multichannel tester is 1 mV and 3 mA. Time interval for data recording was 30 s. Temperature-controlled isothermal experiments were performed in an environmental chamber (circulator oven D045, Deng Yang). Cells were allowed for 3-h rest before commencing test regime at the high temperature.

In the life cycle tests, Cell L was first characterized at 25 °C with a procedure comprises 10 cycles of charge–discharge regime at C/10 and 5 cycles with C/10 charge and C/2 discharge. Cell L was then subjected to 1 C/10 cycle and 100 cycles of C/10 charge and C/2 discharge regime at 60 °C. The end-of-charge (EOC) cutoff condition comprises a typical cutoff voltage at 4.2 V and a capacity limit of 10 Ah. At the end of the life cycle test, 10 additional C/10 cycles were carried out at 60 °C.

Cell P was tested using a different test plan and protocol. A C/10 cycle was conducted first, followed by four cycles of C/10 charge and C/2 discharge regime. Such a five-cycle regime was repeated at 25 and 60 °C.

The data and presentations used in the illustration and discussion in this paper are selected from representative cells in each type that are worth discussion or comparison. Therefore, the results generally reflect the behavior of each type of cells.

3. Results

Fig. 1(a) displays the voltage vs. capacity curves in the first few cycles of Cell L at 25 °C. Little change was observed among the first 15 cycles. The cell delivered 11.35 Ah at C/10 and 11.14 Ah at C/2. Fig. 1(b) shows similar curves in the first 5 cycles of Cell P. The cell delivered a higher capacity with 13.38 Ah at C/10 and 13.07 Ah at C/2.

Although the shape of discharge curves appears similar, Cell P released more capacity in the low voltage range than Cell L. In comparison, below 2.75 V; Cell L delivered 2.5% and 3% capacity at C/10 and C/2, while Cell P delivered 4.5% and 6.5%, respectively.

There is a difference in polarization resistance between the two cells at 25 °C. In Cell L voltage variation between C/10 and C/2 was $\Delta V = 80$ mV, whereas in Cell P it was 100 mV. Using Ohm's law approximation (where a linear polarization was observed in the cell), Cell P exhibited a normalized resistance of 250 mΩ Ah, whereas Cell L was at 200 mΩ Ah. Other cells tested under different test regimes also gave results on the same order of magnitude.

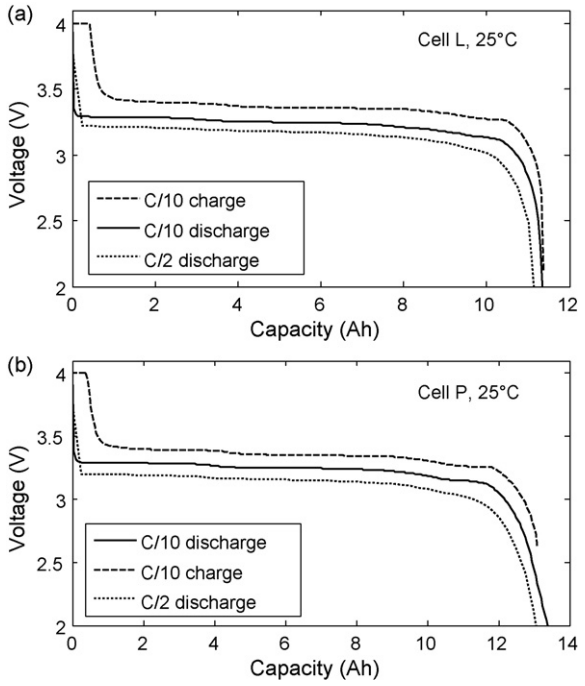

Fig. 1. (a) Voltage–capacity (V vs. Q) curves for Cell L in the first 15 cycles at 25 °C. The cell was charged at C/10 and discharged at C/10 for the first 10 cycles and C/2 for the following 5 cycles. (b) Voltage–capacity curves for Cell P in the first 5 cycles at 25 °C.

Fig. 2 shows the first few discharge regimes in each cell obtained at 60 °C. For both cells, the first discharge regime was at C/10 followed by C/2. Cell L delivered 11.25 Ah (cell was fully charged at C/10 first) at C/10 and 9.9 Ah for the first C/2 discharge, 89% of its capacity at 25 °C. Such low capacity retention at C/2 was due to the capacity cutoff in the charge regime where only 10 Ah were allowed to be recharged. Cell P retained 13.26 Ah (99%) at C/10 and

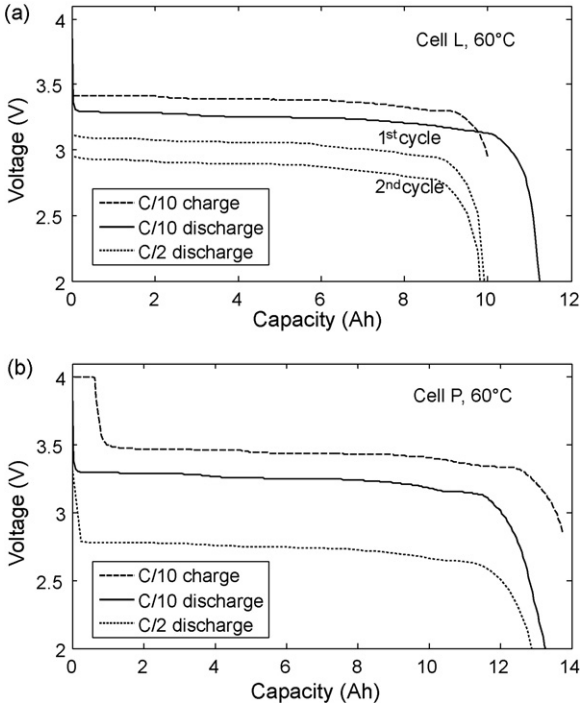

Fig. 2. (a) Cell L voltage evolution upon cycling at 60 °C (100 cycles of C/10 charge and C/2 discharge regime) and (b) capacity evolution vs. cycle number.